# RESEARCH ARTICLE

## ANALYSIS ANDDESIGN OF COOLING CHAMBER FOR GAS ATOMIZATION PLANT

### *Pankaj Sharma

Department of Mechanical Engineering, Dr B R A College of Agril Engg & Tech, Etawah – 206001 (UP), India

| ARTICLE INFO | ABSTRACT |
|---|---|
| | The spray forming process is the process in which a molten metal is impinged by inert gases which results in atomized droplet. The resulting metal droplets while on flight and in residence time inside the spray cone cools rapidly before impinging onto the substrate. The temperature of smaller droplet drops down very fast and strikes the substrate in solid state while larger droplet strike the substrate in liquid form. Therefore to get the mushy droplet impinging on to the substrate knowledge of the thermal history of droplet is of utmost important. In order to determine the size of the cooling chamber of gas atomization plants, a fundamentally based mathematical model was described and the governing differential equation was solved using mathematically modelling method, and the relation between the flight distance and the time was established, then it is solved with the help of initial and boundary condition. With the help of the atomizer angle the size of the cooling chamber is calculated by the help of trigonometry. |

## 1. INTRODUCTION

In recent years spray forming has been an emerging forming process for the production of near net shape products with the benefits that of rapid solidification, semi solid processing etc. This spray forming processes combine the advantage of metal casting and powder metallurgy. Spray forming has minimized the multiple steps of powder metallurgy which includes processes like powder production, sieving, de-gasing and consolidation into a single processing step and still micro-structural characteristics remains the same. Figure 1.1, illustrates the schematic view of spray forming. Professor Singer at the Swansea University first developed the idea of gas atomized spray forming in 1970s in which a high pressure gas jet impinges on a stable melt stream to cause atomization. The resulting droplets are then collected on a target, which can be manipulated within the sprays and used to form a near-dense billet of near-net shapeSpray forming, also known as spray casting, spray deposition is a method of casting near net shape metal components with homogeneous microstructures via the deposition of semi-solid sprayed droplets onto a shaped substrate. In spray forming an alloy is melted, normally in an induction furnace, then the molten metal is slowly poured into a conical tundish into a small-bore ceramic nozzle. The molten metal exits the furnace as a thin free-falling stream and is broken up into droplets by an annular array of gas jets, and these droplets then proceed

downwards, accelerated by the gas jets to impact onto a substrate. 'The process is arranged such that the droplets strike the substrate whilst in the semi-solid condition, this provides sufficient liquid fraction to 'stick' the solid fraction together. Deposition continues, gradually building up a spray formed billets of metal on the substrates. In the spray forming processes the metal is heated in the crucible until the superheat temperature is reached and the molten metal is poured in the tundish. The molten metal stream is poured into the atomization chamber using the gravity, where the molten metal stream gets disintegrated into spherical droplets due to jets of inert gases with very high kinetic energy. The spray thus formed gets accelerated towards the preformed substrate, cools down and solidifies partly as a result of high rate of heat transfer from the spray to the cold inert gas. The diameters of gas atomized droplets varies from 5μm to 500μm. Later on the droplets impacts on to the substrate, merges and forms the deposit. It was in 1960 in Swansea, Wales, by Singer and his colleagues when the first use of metal spray forming was used. In 1970s, spray forming was used as a substitute for conventional forming as production of perform was done directly from the melt. The spray forming process for money-making was first used by a number of singer's young researchers and as a result of which they founded the company Osprey Metals in Neath, Wales. Hence sometimes spray forming process is also called as the Osprey process. Since then, application potentials of the spray forming process has ignited several research and development works at universities and at various industries. In the late '80s Lavernia and Grant

*Corresponding author: Pankaj Sharma,*
Department of Mechanical Engineering, Dr B R A College of Agril Engg & Tech, Etawah – 206001 (UP), India.

developed the liquid dynamic compaction (LDC) process which was similar to spray forming. LDC, Osprey process and spray formings are the generic names of similar or related processes. The purpose of the present work is to determine the sizes of the cooling chamber of gas atomized plants using tools and techniques of mathematical model and solving the mathematical equation by analytical method. The quality and the homogeneity of the microstructures of the deposit and its yield depend on the condition of droplets before impinging and hence it is of the utmost importance to determine and control the conditions and the temperature of the droplets.
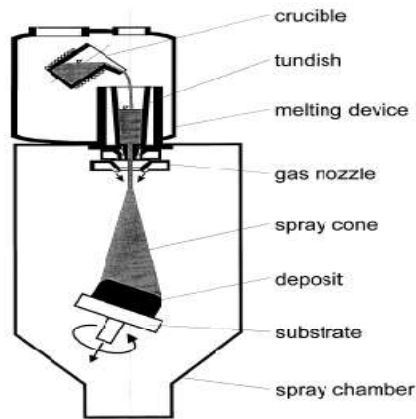


**Fig 1.1. Schematic view of spray forming processes**

## 2. Literature survey

The main intentions of this chapter is to deal with the previous works or researches carried out in the field of spray forming and gas atomized droplets. It has been found that the spray formed materials has many significance over conventional forming processes and the advantages are stated as under:-

- Absence of macro-segregation.
- Homogenous microstructures.
- Increased yield strengths.
- Decreased oxygen contaminants.
- Increased in workability and deformability.

### 2.1 Subdivision of spray forming processes

From the process technology view point spray forming is divided into many sub processes. The subdivision of the complete spray forming is shown in Fig 2.1.
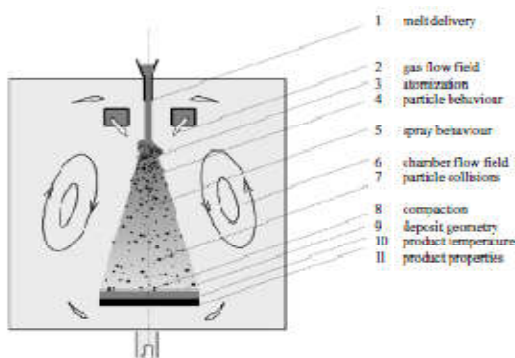


**Fig 2.1. Sub process view of spray forming**

The spray structure consists of in-flight accelerated, thus cooled and partially solidified, melt droplets as well as rapidly heated and decelerated gas flow. Analysis of individual droplet is done to know the behavior regarding movement and cooling of the droplet.

**Ojha *et al.* 1992** described the reason of why analysis of droplet is done before they impinge onto the substrate and is shown as under:-

**Table 2.1. Interaction of preform surface condition and spray condition in controlling the sticking efficiency**



Lawley *et al* (1990) and Mathur *et al.* (1991) have inspected the spray forming process, and have discovered how fundamental knowledge of atomization and the compaction processes affect the system construction. In this way it was found that the appropriate control of processes parameters, such as substrate movements, sprays oscillation, deposit temperature and so on is must, as shown in Figure 2.2. This diagram consists of process that can be controlled by operator on the left side and processes that cannot be controlled by operator directly and the bottom consist of the spray conditions at impact and the surface conditions of the substrate/deposit.

The main purpose of Lawley *et al.*'s and Mathur *et al.*'s was to know parameter that can be controlled and they found that the significant parameters are

- Geometry and dimension of deposits
- The microstructures of the final product (porosity and grain size).

In his work, **Ottosen (1993)** identified the main function in analysis of an integral spray forming model was the modeling and simulation of complex heat transfer and momentum exchange processes.

**Bauckhage and Uhlenwinkel (1996)** laid emphasis on automated and optimized spray forming process, by dividing the spray formings in 3 parts which are melting and atomization, particles transport in spray and compaction.

The process parameters and product quality was linked by **Payne *et al.* (1993)** by the empirical spray forming process model. For suitable process control, Payne *et al* has recognized:

- Process parameters controlled directly: e.g. spray time, melt temperature and GMR;
- Indirectly controllable process parameters: e.g. exhaust gas temperatures, deposit surfaces, roughness and porosity.
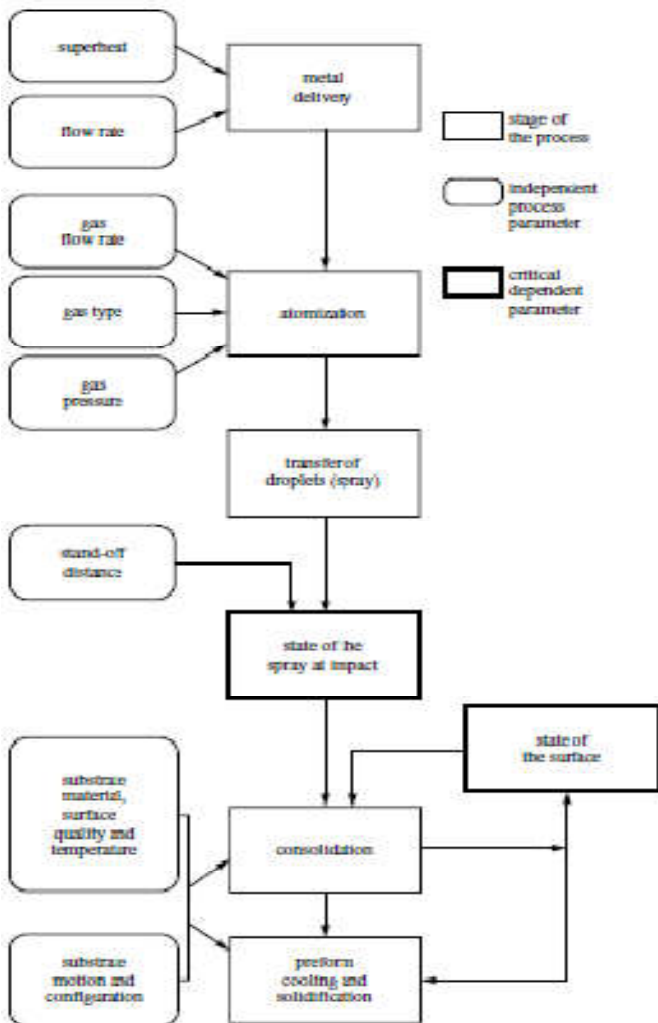


**Fig. 2.2. Modelling of independent and dependent process parameters**

The multi-coupled simulation of turbulent dispersed multiphase flow, containing gas as a continuous phase and droplets as a dispersed phase, is based on two modeling concepts:

- Eulerian/Lagrangians approach

This approach is related to direct intuitive approach which is applied in the analysis of the behavior of dispersed multiphase flow. In this individual particle is under the scanner of study and its interaction with local surroundings are analyzed on the scale of droplets size. Crowe *et al* (1977), Grant *et al* (1993), Bergmann *et al* (1995) were the researchers who published several models within spray formings application based on this approaches.

- Eulerian/Eulerians approach

In this the dispersed phase is considered to be as a quasi-second fluid with spatially averaged properties. Based on this approach derivation of the spray structure within the spray forming process has been done by Liu (1990) and Fritsching *et al.* (1991).

**2.2 Particle Movement**

A fundamental description of the behavior of droplets in gas, the flow around gas atomized droplets and their analysis is given in Clift et al (1978), Crowe et al (1998), Sadhal et al (1997) and Sirignano (1999).

The various forces exerted on individual spherical particles are listed in Table 2.2.

**Table 2.2. Various forces exerted on individual spherical particles**

| | |
|---|---|
| (1) inertial force | $F_i = -\rho_p V \dfrac{dv_p}{dt}$ |
| (2) field force | |
| • gravity force | $F_g = \rho_p V g$ |
| (3) pressure forces | |
| • buoyancy force | $F_a = -\rho_g V g$ |
| • pressure gradients | $F_p = -\rho_g \dfrac{dv_g}{dt} V$ |
| (4) fluid mechanics forces | |
| • resistance force | $F_w = -\dfrac{1}{2}\rho_g A_p c_w(Re)|v_p - v_g|(v_p - v_g)$ |
| • added mass | $F_n = -\dfrac{1}{2}\rho_g V \left(\dfrac{dv_p}{dt} - \dfrac{dv_g}{dt}\right)$ |
| (5) other forces | |
| • Basset history integral | $F_b = \dfrac{3}{2}d^2 \sqrt{\dfrac{\rho_g \mu}{\pi}} \left( \int_{=\infty}^{t} \dfrac{\frac{du_p}{dt} - \frac{du_g}{dt}}{(t-\tau)^{1/2}} d\tau + \dfrac{(u_p - u_g)_{t_0}}{\sqrt{t}} \right)$ |

The spherical droplet trajectory is derived from: ∑F=O

The added-mass term describes the involvement of the surrounding gas, which gets accelerated together with the particle in the boundary layer of the particle. The last term of Basset history integral has been discovered by Reeks and McKee (1984) for the finite particle starting velocity.
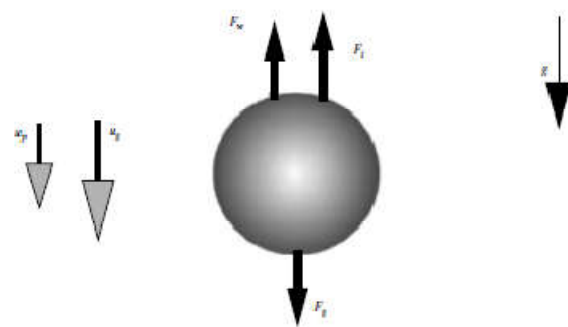


**Fig. 2.3. Coordinate system for force-balancing for spherical droplet**

In the analysis of gas atomized droplets, the density ratio of gas to the particles is negligible ($\rho_g/\rho_p < 10^{-3}$). The particle trajectory equation can be simplified:

$$m_p \frac{d\mathbf{u}_p}{dt} = m_p \mathbf{g} + \frac{1}{2}\rho_g |\mathbf{u}_g - \mathbf{u}_p|(\mathbf{u}_g - \mathbf{u}_p) c_d A_p. \tag{2.1}$$

The force balance taken into account are force due to inertia, gravity and resistance. The resistance drag force coefficients $c_d$ is described in the range of Reynolds number.

Re < 800

$$c_d = \frac{24}{Re}(1 + 0.15Re^{0.687}), \quad Re < 800.$$

(2.2)

**Cliff *et al* (1978)** found that in the area of stokes flow Re <1,

$$c_d = \frac{24}{Re}\left(\frac{1 + \frac{2}{3}\overline{\mu}}{1 + \overline{\mu}}\right), \quad Re < 1.$$

(2.3)

**Mahesh *et al* (2002)** investigated the influences of dynamics of the droplets and temperature variations on the microstructures of final products. For this analytical models were constructed taking into consideration higher Reynolds number leading to supersonic flow of gases. The nozzles were designed so as to develop Mach no 3. Figure 2.4 describes the variation of velocity profile with flight distance. At first gas velocity gas substituted as 1000 m/s. and gas velocity had an inverse relation with the flight distance and was fond to be 200 m/s at 0.7 m.We found the atomized gas velocitybut taking a leap further. Instead of considering gas velocity as an average we opt to consider instantaneous velocity. Which would obviously be more appropriate?
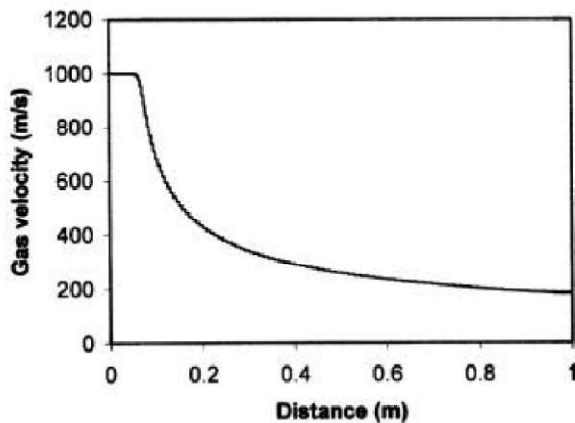


**Fig. 2.4 Variation of gas velocity with respect to the flight distance**

Fig. 2.4 shows the relation b/w flight distance, Reynolds's no., droplet sizeconsidering the velocity of the droplet relative to the gas. Reynolds's number is more predictable for the larger sized droplet.   $Re = \rho.u.d/\mu$
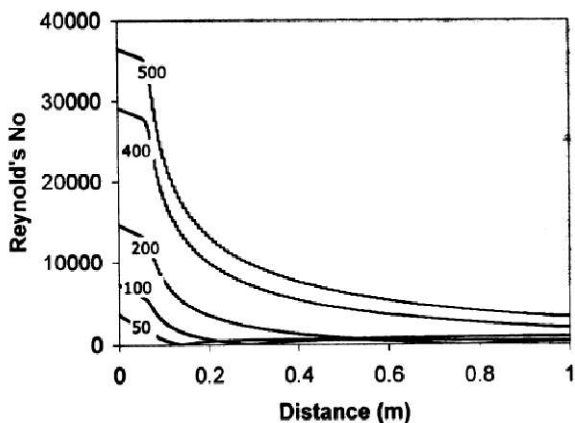


**Fig 2.5. Variation of Reynolds number for different droplet size**

Figure 2.6 shows the droplet's and gas velocity profile for varying sized droplets with respect to flight distance. It is obvious from the graph that at the exit of the nozzle the droplets have very less velocity (equal to acceleration due togravity) and during the flight they gain velocity owingto the momentum transfer from the atomizing gases. Thesmallest droplet attains highest velocity duringthe flight and *vice versa*. The relative velocity of gas and droplet becomes zero as the flight distance increasesand is equivalent to Reynold numbers variation.
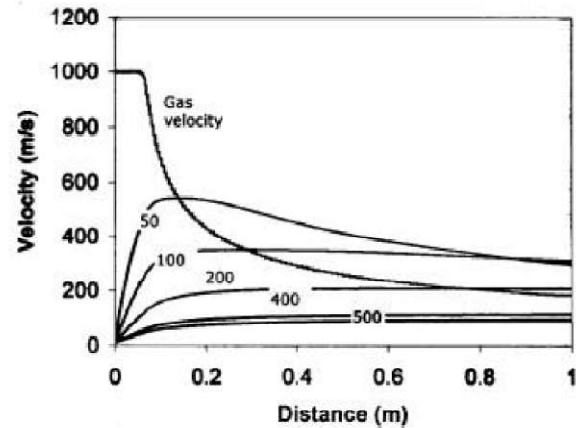


**Fig. 2.6. Droplet's and Gas Velocity Profile for Varying Sized Droplets With respect to Flight Distances**

The smaller droplets moves faster than atomizing gas and attain maximum velocity in minimum time. As the Reynolds number for smaller droplets are extremely small, counterintutively large sized droplets had their drag coeff. Remaining more or less constant because of higher inertia where as for smaller droplets velocity varied considerably totheir high inertia forces and thus no deceleration happens. Mostly droplets have a high velocity of the order of 100 m/s. the cooling mechanism of dendrites is explained on the basis of dendrite formation.

## 2.3 Heat transfer and Cooling of the droplet

The microstructure and the properties of sprayedalloy or of the final product can be known approximately by calculatingthe droplet thermal histories.The cooling due to convection is largely responsibles for heat transfer in metal droplets because of a largetemperature differences between molten metal droplets andcool atomizing gas. As a result for liquid metal droplets during atomization, convective cooling dominates over radiative coolingand hence radiation effect can be neglected (Lavernia *et al.,* 1988; Mathur *et al.,* 1989; Grant *et al.,* 1993; Eon-Sik Lee and Ahn, 1994). However, since the heatextractions from a droplets surface depends on the relativevelocity between the cooling gas and the droplet itself, itis necessary to estimate droplet and gas velocities as discussedby Lavernia *et al.* (1988). Most of the researchers have adopted lumped parameter models (LPM) for calculation of heat transfer in gas atomized droplets (Lavernia *et al.,* 1988; Mathur *et al.,* 1988; Gutierrez *et al.,* 1989; Grantt *et al.,* 1993; Eon-Sik Lee and Ahhn 1994; Dimos and John, 1997). Moreover, Levi and Mehrabian (1982) shows that LPM give needed results when the temperature gradient inside the droplet is very large. The LPM is used for the simplicity of computation, since only first order ordinarydifferentials equations are to be solved. The small size ofthe dropletsplay a

significant role in neglecting theheat conduction within the droplets i.e. The droplet temperature is considered uniform (Lavernia *et al.,* 1988; Grant *et al.,* 1993; Eon/Sik Lee and Ahn, 1994). The process ofconduction freezing using LPM as well as radially symmetric non-isothermal models have been analyzedby (Bayazitoglu and Cerny, 1993). In this not only the radial symmetry was imposed on the droplet but also the presence of recalescence resulting from severe undercoolings and phenomena of non-equilibrium was neglected. The LPM is accurate and also the assumption of uniform temperature inside the droplet is justified when the cooling rate was 104K/s. This follows the Newtonian cooling and gives rise to LPM.

**Equating the rate of change of sensible heat for the droplet to the rate of heat radiated from the surface. (Lavernia *et al.,* 1988),**

$$m_p c_p \frac{\mathrm{d}T_p}{\mathrm{d}t} = \mathrm{Nu}\lambda_g \pi \mathrm{d}_p (T_g - T_p) \tag{2.4}$$

Equation (2.4) is to be integrated. But heat transfer coefficients could not be considered to be a constant since the velocity of the gas decreases andthat of the droplets increases. Neglecting radiation heat exchange and employing equation. (Ranzz and Marshal, 1952)

$$\mathrm{Nu} = 2 + 0.6\mathrm{Re}^{0.5}\mathrm{Pr}^{0.33} \tag{2.5}$$

$$P_r = \frac{C_g \mu_g}{K_g} \tag{2.6}$$

Where, $C$g is the gas specific heat, $\mu_g$ the absolute viscosityof gas and $K_g$ the gas thermal conductivity

Equation (2.5) has Nusslet no. that depends on the dia. Of the droplet and prandtl no. which is a function of the upstream flow conditions, reynold's no. here which is alo a part of the eq. depends on the flow vel. Here (Lavernia *et al.,* 1988; Mathur*et al.,* 1989; Grant *et al.,* 1993; Eon/Sik Lee and Ahn 1994) has limited validity (Dimos and John, 1997). As the Ranz and Marshall's correlation for '*h*' is correct when the Reynoldsnumber lies in the range of 0.1 to 4000. For supersonic gas atomization when Re. is more than 4000 Whitaker's (1972) correlation is used:

$$N_u = \frac{hD}{K} = 2 + \left(0\cdot 4\mathrm{Re}^{1/2} + 0\cdot 06\mathrm{Re}^{2/3}\right)\mathrm{Pr}^{0\cdot 4}\left(\frac{\mu_\infty}{\mu_s}\right)^{1/4} \tag{2.7}$$

Heat transfer coefficient with the function of flight distanced is to be known first before predicting the thermal states of droplets. For this Whitaker's correlation employed spherical surface considerations. From figure 7 it evident that smaller droplets have higher coefficient of heat transfer due to higher surface area to volume ratio. The droplet history can be known Thereby

Figure 2.8 shows temperature variation for differentdroplet sizes as a functions of flight distance. The solidus and liquidus temperature are illustrated to identify the physical state of the droplets based on their size when they reach the substrate. We know that mushy dropletsprovide best quality preform hence it

is important to know which droplet size strike the substrate in mushy zone and it was done by determining solid fraction of droplet.
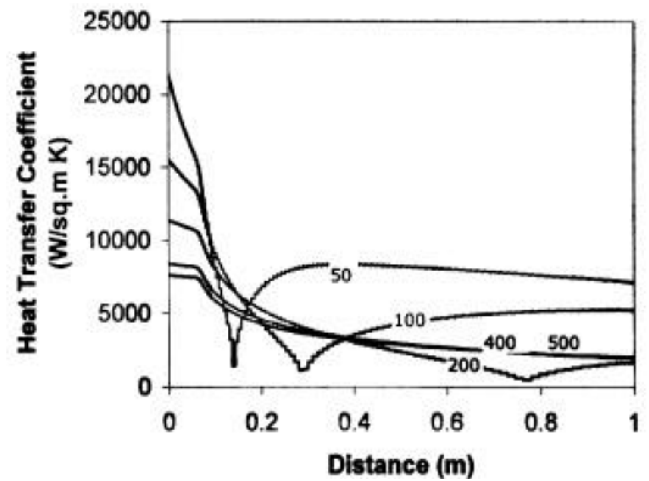


**Fig. 2.7. The variations in heat transfer coefficients for different droplet size with the flight distance**
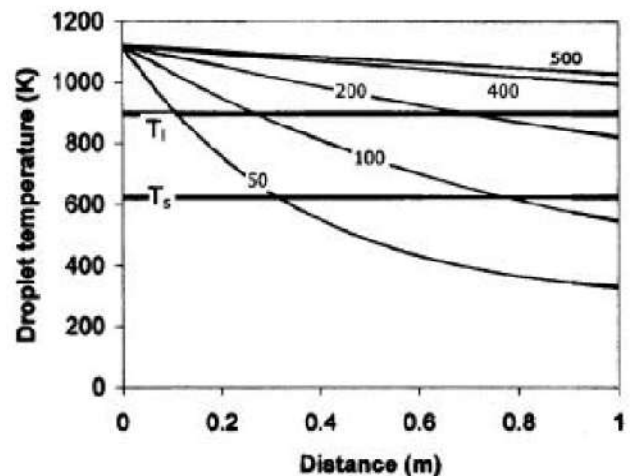


**Fig. 2.8. Temperature variation for different droplet sizes as a function of flight distances**

Figure 2.9 depicts percentage of solid in the droplets versus flight distance. It is seen from the figure that smaller droplets solidify completely at a distance from 0.2 to 0.6 m. The droplets of more than that of 100 µm sizes would be in semisolid/semi liquid state for a longer time. This analysis helps in optimizing the stand-off distances for given set of atomization parametersand for a particular metal and its alloys system. From this analysis it was found that the standoff distance of 0.6 to 0.7 m is suitable forobtaining preform in Al–Si–Mg alloy during the depositiontrials. At this standoff distance it was anticipated thatthe droplets of size variety between 100 and 500 µm possesses 90% to 15% solid fractions respectively. The parameters in spray casting be set up in such a way that the sprayhas more volume fraction of mushy droplets i.e. the droplets of size around 200–300 µm.

Figure 2.10 shows the rate of cooling in the droplets. From the figures it is evident that the cooling rate is very high for almost all the sizes of droplets. Cooling rate for smaller droplets were more as they lose heat faster.
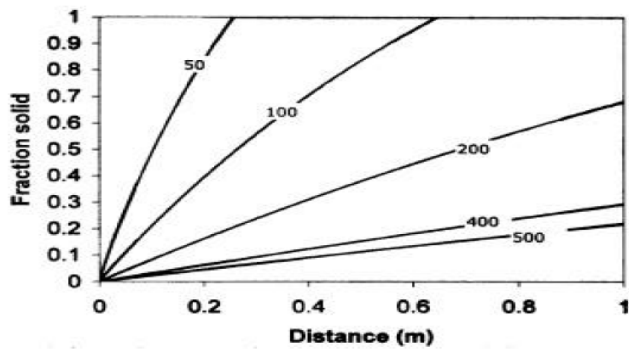
**Fig. 2.9. Percentage of solid in the droplets versus flight distances**
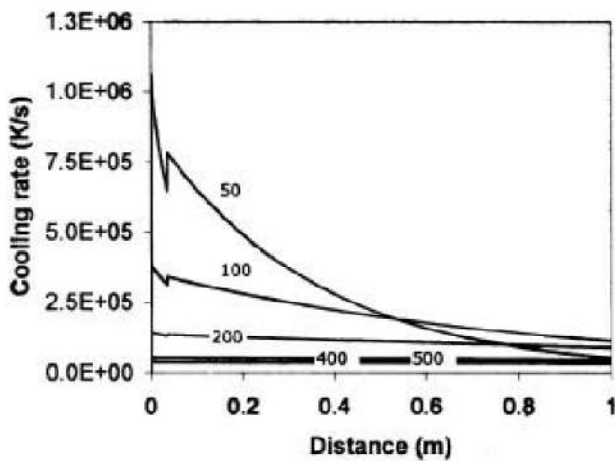


**Fig 2.10. The rate of cooling in the droplets**

## 2.4 Solidificationsof gas atomized droplets

Nucleation and growth of the crystal describes the solidification behavior of gas atomized droplets. Initially the solidification process is described by a homogeneous nucleation with slow cooling rates and thus without under-cooling for pure metals. Here it is implicit that the superheated meltdroplet while cooling to the phase change temperature releases the latent heat and transfers it across the surface. After solidification the particlemass cools down further. In the heterogeneous cooling model the foreign particles initiate the cooling process. In this model, uponreaching the solidification temperature, a balance exists between the released latent heatand the heat convectively transferred across the surface of the droplet and thus the temperature ofthe droplet remains constant during solidification. These solidification models have beenused in spray forming, for example, by Zhang (1994) and Liu (1990). The solidification model described here (Bergmann, 2000) was developed for lowcarbonsteel C30 (0.30 wt. % C), but may be easily adapted to other material compositions. The solidification model explained here is developed for low carbon steel C30 (0.30 weight% C) but is easily modified to other material compositions. Figure 2.10shows part of the iron-carbon phase diagram, where the area for C30 is marked. For lowcooling rates, temperature with respect to time curve can be drawn using this phasediagram. As in spray forming the cooling rate immediately after atomizations is very high hence there is a chances of undercooling even before the nucleation starts.

Starting with the superheated temperature$T_m$, the droplet cools down to liquidus temperature $T_l$. Ifthe cooling rate is high

droplet may undercool until nucleation starts on reaching the nucleation temperature. As there is release in latent heat of fusion during recalescence, the droplet temperature increases until it reachesa local maximum in the cooling curve at $T_r$. Later on it follows segregated solidification, as the temperature keeps on decreasing. At temperature $T_{per}$, the peritectictransformations takes place at constant droplet temperature. As the peritectic transformation ends up, segregated solidification starts again until the droplet iscompletely solidified at $T_s$. After this in solidified state itself the droplet cooling continues.
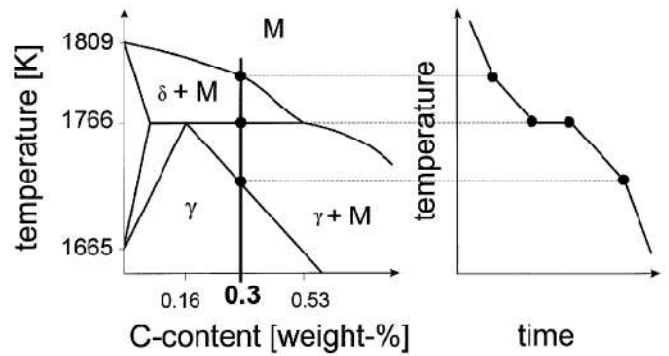


**Fig 2.11. Phase Diagram of the Fe-C and the corresponding variation in phases with time**
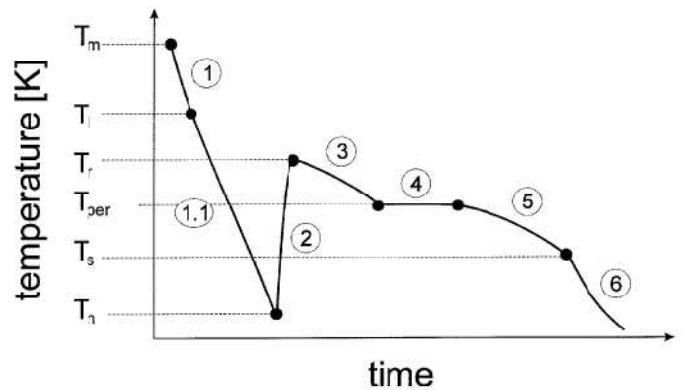


**Fig. 2.12. Temperature variation of gas atomized droplets with respect to time**

Separate analysis of droplet cooling and solidification:

**Cooling in the liquid state**

For a spherical droplet, the change of internal heat content according to convection and radiation heat transfercan be expressed by:

$$c_{d.l}\frac{dT_d}{dt} = -\frac{6h}{\rho_d d_d}(T_d - T_g) - \frac{6\varepsilon\sigma}{\rho_d d_d}(T_d^4 - T_w^4) \quad (2.8)$$

Where

$T_d$= droplet temperature, $T_g$= gas temperatureand $T_w$= temperature of the surrounding walls. The specific heat capacity of the liquid droplet materialis $c_{dl}$; $h$ is the heat transfer coefficient, $\varepsilon$ and$\sigma$ are theemissivity and Stefan–Boltzmann constants, $\rho_d$ and $d_d$ arethe droplet's density and diameter, respectively.

## Undercooling

The solidification process does not start immediately after liquidus temperature but the solidification depends on the cooling rate and on the size of the droplet. Nucleation temperature can be much lower than the liquidus temperature. The nucleationtemperature for continuous cooling is defined as the temperature, where the number of nuclei $N_n$ in the dropletvolume $V_d$ is identical to one:

$$N_{\mathrm{n}} = V_{\mathrm{d}} \int_{T_1}^{T_{\mathrm{n}}} \frac{J(T)}{\dot{T}}\, \mathrm{d}T = 1 \tag{2.9}$$

Heterogeneousnucleation minimizes the degree of undercooling. Themaximum undercooling for iron based alloys is 295 Kelvin and a minimum undercooling of 3 Kelvin is assumed.

## Recalescence

As the solidification starts there is an increase in the temperature of droplet due to release of latent heat of fusion. The conservation equation forthe droplet thermal energy is extended to:

$$c_{\mathrm{d}} \frac{\mathrm{d}T_{\mathrm{d}}}{\mathrm{d}t} = \Delta h_{\mathrm{f}} \frac{\mathrm{d}f_{\mathrm{s}}}{\mathrm{d}t} - \frac{6h}{\rho_{\mathrm{d}} d_{\mathrm{d}}}(T_{\mathrm{d}} - T_{\mathrm{g}}) - \frac{6\varepsilon\sigma}{\rho_{\mathrm{d}} d_{\mathrm{d}}}(T_{\mathrm{d}}^4 - T_{\mathrm{w}}^4) \tag{2.10}$$

with $f_s$ as fraction solid ($f_s$= O droplet is completelyliquid; $f_s$=1droplet is completely solid) and thespecific heat capacity of the droplets$c_d$ as the average ofthe solid and liquid contents:

$$c_{\mathrm{d}} = f_{\mathrm{s}} c_{\mathrm{ds}} + (1 - f_{\mathrm{s}}) c_{\mathrm{dl}} \tag{2.11}$$

The phase of recalescence ends, when the production rate of internal heat equals the heat transferfrom the droplets surface. Here, the cooling curve ofa droplets reaches a local maximum and thedroplet temperature equals $T_r$:

$$\Delta h_{\mathrm{f}} \frac{\mathrm{d}f_{\mathrm{s}}}{\mathrm{d}t} = \frac{6h}{\rho_{\mathrm{d}} d_{\mathrm{d}}}(T_{\mathrm{r}} - T_{\mathrm{g}}) + \frac{6\varepsilon\sigma}{\rho_{\mathrm{d}} d_{\mathrm{d}}}(T_{\mathrm{r}}^4 - T_{\mathrm{w}}^4) \tag{2.12}$$

## Segregated solidification 1

The heat conservation equation in this stage is described by

$$\frac{\mathrm{d}T_{\mathrm{d}}}{\mathrm{d}t}\left(c_{\mathrm{d}} + \Delta h_{\mathrm{f}} \frac{\mathrm{d}f_{\mathrm{s}}}{\mathrm{d}T_{\mathrm{d}}}\right)$$
$$= -\frac{6h}{\rho_{\mathrm{d}} d_{\mathrm{d}}}(T_{\mathrm{d}} - T_{\mathrm{g}}) - \frac{6\varepsilon\sigma}{\rho_{\mathrm{d}} d_{\mathrm{d}}}(T_{\mathrm{d}}^4 - T_{\mathrm{w}}^4) \tag{2.13}$$

## Peritectic transformation

When the droplet temperature reaches the peritectictemperature, it remains at a constant value until this phase transformation got completed. The change in solid fractionduring peritectic solidification is described by:

$$\Delta h_{\mathrm{f}} \frac{\mathrm{d}f_{\mathrm{s}}}{\mathrm{d}t} = -\frac{6h}{\rho_{\mathrm{d}} d_{\mathrm{d}}}(T_{\mathrm{d}} - T_{\mathrm{g}}) - \frac{6\varepsilon\sigma}{\rho_{\mathrm{d}} d_{\mathrm{d}}}(T_{\mathrm{d}}^4 - T_{\mathrm{w}}^4) \tag{2.14}$$

Peritectic solidification gets completed, when the composition ofthe remaining liquid reaches the appropriate concentration.

## Segregated solidification 2

Segregated solidification again comeinto picture after peritectic transformation.

## Cooling in the solid state

Further cooling of droplet takes place after solidification. This process can beevaluated from the following equation:

$$c_{\mathrm{ds}} \frac{\mathrm{d}T_{\mathrm{d}}}{\mathrm{d}t} = -\frac{6h}{\rho_{\mathrm{d}} d_{\mathrm{d}}}(T_{\mathrm{d}} - T_{\mathrm{g}}) - \frac{6\varepsilon\sigma}{\rho_{\mathrm{d}} d_{\mathrm{d}}}(T_{\mathrm{d}}^4 - T_{\mathrm{w}}^4) \tag{2.15}$$

with$c_{ds}$ as the specific heat capacity of the solid materials.

## Solidification behavior inside the melt particles

The temperature variation inside a single spherical droplet during solidification has beenstudied numerically by Kallien (1988) and Hartmann (1990). The simulation program was developed for solidification during metals casting. It includes undercooling thus calculates three-dimensional temperature variation in gas atomized droplet. The model is based on Fourier law for transient heat conduction in three-plane (Cartesian) coordinates as-

$$\rho c_p \frac{\partial T}{\partial t} = \frac{\partial}{\partial x}\left(\lambda \frac{\partial T}{\partial x}\right) + \frac{\partial}{\partial y}\left(\lambda \frac{\partial T}{\partial y}\right) + \frac{\partial}{\partial z}\left(\lambda \frac{\partial T}{\partial z}\right) \tag{2.16}$$

where conductivity $\lambda$, density $\rho$ and heat capacity $c_p$, dependon location and temperature.

A modified temperature is introduced to achieve linear differentials equation.

$$\Theta = \frac{1}{\lambda_0} \int_0^T \lambda\, \mathrm{d}T \tag{2.17}$$

and thus linear differential equation was :

$$\frac{\rho c_p}{\lambda_0} \frac{\partial T}{\partial t} = \frac{\partial^2 \Theta}{\partial x^2} + \frac{\partial^2 \Theta}{\partial y^2} + \frac{\partial^2 \Theta}{\partial z^2} \tag{2.18}$$

Finite difference method was used to solve this equation on an orthogonal-plane three dimensional grid.

The assumed boundary conditions are:

- The surrounding gas is assumed to be at constant temperature,
- Constant heat transfer coefficients across the whole surface of the droplet.
- At preselected nucleation temperature the solidification was initiated and nucleation was

considered to take place at either at single point or at number of grid cells.

A six stages approach for the particle solidification was assumed:

(1) Cooling of the melts from superheating until the nucleation temperature is reached,
(2) Attaining the highest undercoolings,
(3) Solidification and recalescence,
(4) Cooling and solidification in the melt temperature range between solidus and liquidus,
(5) end of solidifications,
(6) Cooling of the solidified particles.

For the recalescence phase, the releasing velocity of latent heat depend on undercooling $\Delta T$:

$$v = K\Delta T$$

As soon as the grid cells solidifies completely the adjacent cells begin to release the latent heat. Degree of undercooling controls the velocity of solidification. The heat transfer coefficient was taken as h= 20 000 W/m$^2$ K and theundercooling prior to nucleationswas considered to be 50 K. The solidification process initiates at a single point on the surface of the particle in a plane inside the particles. As there is release of latent heat, the interior of the particle gets heated up. For a 10% solidification rate, movement ofthe solidification front is visible, which raises the temperature of the surrounding grid cellsclose to the liquidus temperature. As Biot number is very less temperature variation inside the spherical droplets are neglected. Thus this behavior necessitates for refined modeling in order to obtain realistic spray formingsmodeling results.

## 3. Mathematical modelling

The modeling to determine the size of the gas atomized plant is done using fundamentally based mathematical model. Mathematical models are a set of trigonometry equations which represents a process or some aspect of it. Mathematical models have lots of merits over other modeling for e.g. no data is required, knowledge of mechanism of process is a must and there is no limit to these models as they can be applied anywhere.

### 3.1 Development of fundamentally based mathematical model

- Preparation
- Mathematical formulation
  1. Assumptions
  2. The balance (force)
  3. Initial and boundary condition
- Solution of mathematical equations
  1. Analytical method
- Validation of model.

### 3.2 Preparation

The parameter which is to be calculated is the size of the gas atomization plant which is a function radius r,and the atomizer angla. That means the complexity of the model is the two dimensional state. Here aluminium alloys are taken into consideration

**Table 3.1. Thermophysical properties of pure Aluminium**

| Diameter of the droplets (dd) | 20, 40, 60, 80, 100, 120, 140,160 μm | Melting tem.(T$_m$) | 933 K |
|---|---|---|---|
| Density($\rho_d$) | 2.707 g/cm$^3$ | thermal diffusivity($\alpha$) | 8.418*10$^5$ m$^2$/s |
| Thermal conductivity(k$_a$) | 204 W/m-K | Undercooling | 50K |

**Table 3.2. Properties of Nitrogen Gas**

| Specific heat(C$_{pg}$) | 1039 J/kg-K |
|---|---|
| Thermal conductivity(k$_g$) | 2.6 *10$^{-2}$ W/m-K |
| Dynamic viscosity($\mu_g$) | 1.78*10$^{-5}$ Ns/m$^2$ |
| Density($\rho_g$) | 0.808 g/cm$^3$ |

## 3.3 Mathematical Formulation

### 3.3.1 Assumption

- Property remains constant i.e., metal is homogenous and isotropic.
- No heat generation inside the spherical droplet.
- Surrounding gas atmosphere is assumed to be at constant temperature which is taken to be at 0temperatures.
- The heat transfer coefficient is taken as constant across the whole surface of the particle.
- Homogeneous solidification occurs in the particle.
- There is no heat loss due to radiation.
- The Lumped Parameter Model used earlier by several researchers has not been taken into consideration.
- Droplets are considered to be perfectly spherical in shape with no deformation.
- There is no scattering or diffusion of the droplets.
- The added-mass term describes the involvement of the surrounding gas, which gets accelerated together with the particle in the boundary layer of the particle.

### 3.3.2 The Balance

The spherical droplet trajectory is derived from: $\sum F = ma$

$$m_p\frac{\partial U_p}{\partial t} = m_p g + \frac{1}{2}p_g I u_g - u_p I \,(u_g - u_p)C_d A_p$$

$$m_p\frac{\partial^2 h}{\partial t^2} = m_p g + \frac{1}{2}p_g I u_g - u_p I \,(u_g - u_p)C_d A_p$$

$$\text{where} A_p = \frac{\pi}{4}d^2$$
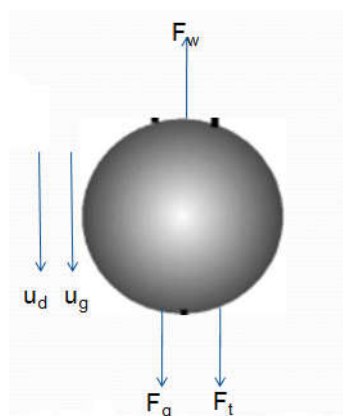


**Fig. 3.1. Balancing of forces on the droplet**

## 3.4 Solution of mathematical equations

Cd is given by $0.28 + \frac{6\sqrt{Re} + 21}{Re}$

Where Re is the reynold no. and is given by

$Re = \frac{pgdIug-upI}{\mu}$ where $\mu$ is the gas dynamic viscosity

**Table 3.3. For the calculation of the mass of the particles:**

$$M_p = p_{p*} V_p$$

| Diameter of particle(d in μm) | Density of particle($p_p$ in g/ cm³) | Volume of particle(cm³*10⁻⁹) $V_p = \frac{\pi}{6}d^3$ | Mass of particle($m_p$ in gm*10⁻⁹) |
|---|---|---|---|
| 20 | 2.7 | 4.186667 | 11.2500 |
| 40 | 2.7 | 33.49333 | 90.4319 |
| 60 | 2.7 | 113.040 | 305.2080 |
| 80 | 2.7 | 267.9467 | 1412.9991 |
| 100 | 2.7 | 523.3333 | 1412.9991 |
| 120 | 2.7 | 904.320 | 2441.6640 |
| 140 | 2.7 | 1436.027 | 3877.2729 |

## Table 3.4

### For evaluating reynold no.(Re)

**Reynold number:** The Reynolds number is defined as the ratio of inertial forces to viscous forces and consequently quantifies the relative importance of these two types of forces for given flow conditions. It is given by:

$$Re = \frac{pgdIug-upI}{\mu}$$

| Density of particle ($p_g$ in g/ cm³) | Diameter of particle (d in μm) | Velocity of gas ($u_g$ in m/s) | Velocity of particle ($u_p$ in m/s) | Gas dynamic viscosity (μ in Pa-s* 10⁻⁵) | Reynold no.(Re *10²) |
|---|---|---|---|---|---|
| 0.808 | 20 | 980 | 228 | 3.78 | 3214.899 |
| 0.808 | 40 | 980 | 177 | 3.78 | 6865.862 |
| 0.808 | 60 | 980 | 150 | 3.78 | 10645.08 |
| 0.808 | 80 | 980 | 134 | 3.78 | 14467.05 |
| 0.808 | 100 | 980 | 122 | 3.78 | 18340.32 |
| 0.808 | 120 | 980 | 112 | 3.78 | 22264.89 |
| 0.808 | 140 | 980 | 105 | 3.78 | 3214.899 |

## Table 3.5

### Calculation of the drag coefficients:

**Drag coefficient:** In fluid dynamics, the drag coefficient (commonly denoted as $c_d$) is a dimensionless quantity that is used to quantify the drag or resistance of an object in a fluid environment, such as atomizing gas or water.

$$C_d = 0.28 + \frac{6\sqrt{Re} + 21}{Re}$$

| Reynold no.(Re) | Drag coefficients(Cd) |
|---|---|
| 321489.9 | 0.010648187 |
| 686586.2 | 0.00727208 |
| 1064508 | 0.005835353 |
| 1446705 | 0.00500311 |
| 1834032 | 0.004442053 |
| 2226489 | 0.004030622 |

## Table 3.6

**Table for evaluating flight distance h:** The flight distance is calculated by the help of intial and boundry condition into the balance equation

$m_p \frac{\partial Up}{\partial t} = m_p g + \frac{1}{2} p_g Iu_g-u_pI \ (u_g-u_p) C_d A_p$

we know that $\frac{\partial Up}{\partial t} = \frac{\partial^2 h}{\partial t^2}$ so

$m_p \frac{\partial^2 h}{\partial t^2} = m_p g + \frac{1}{2} p_g Iu_g-u_pI \ (u_g-u_p) C_d A_p$

by integrating and putting initial and boundry condition at t=0, h=0 and at t=0, v= $v_{max}$ that gives

$h = gt^2 + (\frac{1}{2} p_g (u_g-u_p)^2 C_d A_p \ t^2)/ m_p + v_{max} t$

| Mass of particle ($m_p$ in gm) | Diameter of particle(d in μm) | Cross sectional area ($A_p$ μm²) | Density of particle($p_g$ in g/ cm³) | Velocity of gas ($u_g$ m/s) | Velocity of particle ($u_p$) | Flight distance (h in cm) |
|---|---|---|---|---|---|---|
| 4186.667 | 20 | 314 | 0.808 | 980 | 228 | 15.33 |
| 33493.33 | 40 | 1256 | 0.808 | 980 | 177 | 28.8 |
| 113040 | 60 | 2826 | 0.808 | 980 | 150 | 35.26 |
| 267946.7 | 100 | 5024 | 0.808 | 980 | 134 | 40.94 |
| 523333.3 | 120 | 7850 | 0.808 | 980 | 122 | 44.1 |
| 904320 | 140 | 11304 | 0.808 | 980 | 112 | 46.28 |
| 1436027 | 160 | 15386 | 0.808 | 980 | 105 | 48.4 |

### 3.4.5. Design of Cooling chamber for gas atomization plant:

The radius of the cooling chamber can be determine by the help of Cooling chamber radius(r) $= h*\tan\theta$

Where h is the flight distance and $\theta$ is the atomizer angle
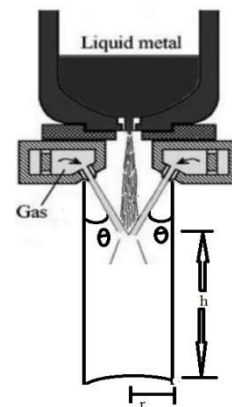


**Fig. 3.2. Design of cooling chamber for gas atomization plant**

### 3.4.5 Calculation for the cooling chamber radius (r) with atomizer angle 35⁰(θ=35⁰)

1. Radius ($r_1$)= 15.33*tan35⁰=10.734 cm
2. Radius ($r_2$)= 28.8*tan35⁰=20.166 cm
3. Radius ($r_3$)= 35.26*tan35⁰=24.689 cm
4. Radius ($r_4$)= 40.94*tan35⁰=28.666 cm
5. Radius ($r_5$)= 44.1*tan35⁰=30.879 cm
6. Radius ($r_6$)= 46.28*tan35⁰=32.406 cm
7. Radius ($r_7$)= 48.4*tan35⁰=33.89 cm

### 3.4.6 Calculation for the cooling chamber radius (r) with atomizer angle 37⁰(θ=37⁰)

1. Radius ($r_1$)= 15.33*tan37⁰=11.552 cm
2. Radius ($r_2$)= 28.8*tan37⁰=21.702 cm
3. Radius ($r_3$)= 35.26*tan37⁰=26.57 cm
4. Radius ($r_4$)= 40.94*tan37⁰=30.85 cm
5. Radius ($r_5$)= 44.1*tan37⁰=33.23 cm
6. Radius ($r_6$)= 46.28*tan37⁰=34.874 cm

7. Radius ($r_7$)= 48.4*tan37$^0$=36.47 cm

### 3.4.6 Calculation for the cooling chamber radius (r) with atomizer angle 39$^0$($\theta$=39$^0$)

1.Radius ($r_1$)= 15.33*tan39$^0$=12.414 cm
2.Radius ($r_2$)= 28.8*tan39$^0$=23.321 cm
3.Radius ($r_3$)= 35.26*tan39$^0$=28.552 cm
4.Radius ($r_4$)= 40.94*tan39$^0$=33.153 cm
5.Radius ($r_5$)= 44.1*tan39$^0$=35.711 cm
6.Radius ($r_6$)= 46.28*tan39$^0$=37.477 cm
7. Radius ($r_7$)= 48.4*tan39$^0$=39.194 cm

### 3.4.7 Calculation for the cooling chamber radius (r) with atomizer angle 41$^0$($\theta$=41$^0$)

1.Radius ($r_1$)= 15.33*tan41$^0$=13.326 cm
2.Radius ($r_2$)= 28.8*tan41$^0$=25.035 cm
3.Radius ($r_3$)= 35.26*tan41$^0$=30.651 cm
4.Radius ($r_4$)= 40.94*tan41$^0$=35.589 cm
5.Radius ($r_5$)= 44.1*tan41$^0$=38.336 cm
6.Radius ($r_6$)= 46.28*tan41$^0$=40.231 cm
7. Radius ($r_6$)= 48.4*tan41$^0$=42.073 cm

### 3.4.8 Calculation for the cooling chamber radius (r) with atomizer angle 43$^0$($\theta$=43$^0$)

1.Radius ($r_1$)= 15.33*tan43$^0$=14.295 cm
2.Radius ($r_2$)= 28.8*tan43$^0$=26.856 cm
3.Radius ($r_3$)= 35.26*tan43$^0$=32.880 cm
4.Radius ($r_4$)= 40.94*tan43$^0$=38.177 cm
5.Radius ($r_5$)= 44.1*tan43$^0$=41.124 cm
6.Radius ($r_6$)= 46.28*tan43$^0$=43.156 cm
7. Radius ($r_6$)= 48.4*tan43$^0$=45.134 cm

### 3.4.9 Calculation for the cooling chamber radius (r) with atomizer angle 45$^0$($\theta$=45$^0$)

1.Radius ($r_1$)= 15.33*tan45$^0$=15.330 cm
2.Radius ($r_2$)= 28.8*tan45$^0$=28.800 cm
3.Radius ($r_3$)= 35.26*tan45$^0$=35.260 cm
4.Radius ($r_4$)= 40.94*tan45$^0$=40.940 cm
5.Radius ($r_5$)= 44.1*tan45$^0$=44.100 cm
6.Radius ($r_6$)= 46.28*tan45$^0$=46.280 cm
7. Radius ($r_6$)= 48.4*tan45$^0$=48.400 cm

### 3.5 Tables for cooling chamber sizes

#### 3.5.1. For atomizer angle 35$^0$($\theta$=35$^0$)

| Flight distance(h in cm) | Cooling chamber size(r in cm) |
|---|---|
| 15.33 | 10.734 |
| 28.8 | 20.166 |
| 35.26 | 24.689 |
| 40.94 | 28.666 |
| 44.1 | 30.879 |
| 46.28 | 32.406 |
| 48.4 | 33.89 |

#### 3.5.2 For atomizer angle 37$^0$($\theta$=37$^0$)

| Flight distance (h in cm) | Cooling chamber size(r in cm) |
|---|---|
| 15.33 | 11.552 |
| 28.8 | 21.702 |
| 35.26 | 26.57 |
| 40.94 | 30.85 |
| 44.1 | 33.23 |
| 46.28 | 34.874 |
| 48.4 | 36.47 |

### 3.5.3 For atomizer angle 39$^0$($\theta$=39$^0$)

| Flight distance(h in cm) | Cooling chamber size(r in cm) |
|---|---|
| 15.33 | 12.414 |
| 28.8 | 23.321 |
| 35.26 | 28.552 |
| 40.94 | 33.153 |
| 44.1 | 35.711 |
| 46.28 | 37.477 |
| 48.4 | 39.194 |

### 3.5.4 For atomizer angle 41$^0$($\theta$=41$^0$)

| Flight distance(h in cm) | Cooling chamber size(r in cm) |
|---|---|
| 15.33 | 13.326 |
| 28.8 | 25.035 |
| 35.26 | 30.651 |
| 40.94 | 35.589 |
| 44.1 | 38.336 |
| 46.28 | 40.231 |
| 48.4 | 42.073 |

### 3.5.5 For atomizer angle 43$^0$($\theta$=43$^0$)

| Flight distance(h in cm) | Cooling chamber size(r in cm) |
|---|---|
| 15.33 | 14.295 |
| 28.8 | 26.856 |
| 35.26 | 32.880 |
| 40.94 | 38.177 |
| 44.1 | 41.124 |
| 46.28 | 43.156 |
| 48.4 | 45.134 |

### 3.5.6 For atomizer angle 45$^0$($\theta$=45$^0$)

| Flight distance(h in cm) | Cooling chamber size (r in cm) |
|---|---|
| 15.33 | 15.330 |
| 28.8 | 28.800 |
| 35.26 | 35.260 |
| 40.94 | 40.940 |
| 44.1 | 44.100 |
| 46.28 | 46.280 |
| 48.4 | 48.400 |

### 4.Analysis and validation

It is obvious from the figure 4.1 that cooling chamber size varies with the respect of the atomizer angle and the flight distance. As Flight distance increases or atomizer angle increases, the size of the cooling chamber also increase and vice versa.
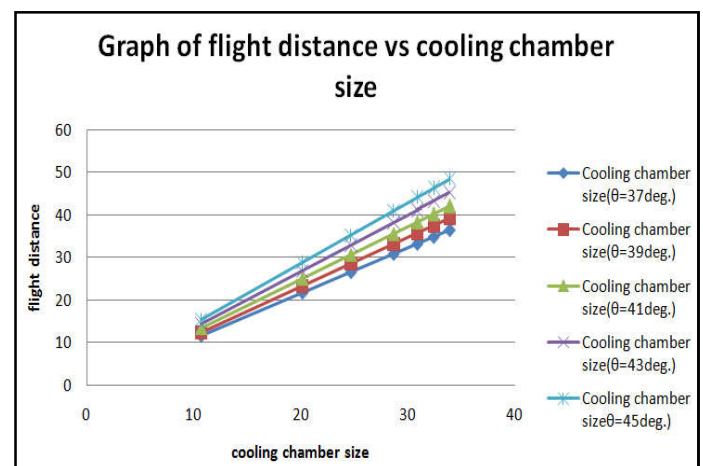


**Figure 4.1**

**Table 4.1**

The Table 4.1 shows the value of temperature for different droplet sizes as a function of time.

| t (in sec) | Temp. in Kelvin for r=20μm | Temp. in Kelvin for r=40μm | Temp. in Kelvin for r=60μm | Temp. in Kelvin for r=80μm | Temp. in Kelvin for r=100μm |
|---|---|---|---|---|---|
| 0 | 1147 | 1147 | 1147 | 1147 | 1147 |
| 0.004 | 660.4770328 | 744.6765096 | 826.2845 | 895.0959 | 913.1761 |
| 0.008 | 380.3225029 | 483.4726276 | 595.245 | 698.5149 | 727.0188 |
| 0.012 | 219.0011144 | 313.8890225 | 428.8071 | 545.1071 | 578.811 |
| 0.016 | 126.107416 | 203.7888245 | 308.9073 | 425.3907 | 460.8164 |
| 0.02 | 72.61643588 | 132.3075418 | 222.5329 | 331.9664 | 366.8758 |

Figure 4.2 shows the temperature variation in gas atomized droplets as a function of time.
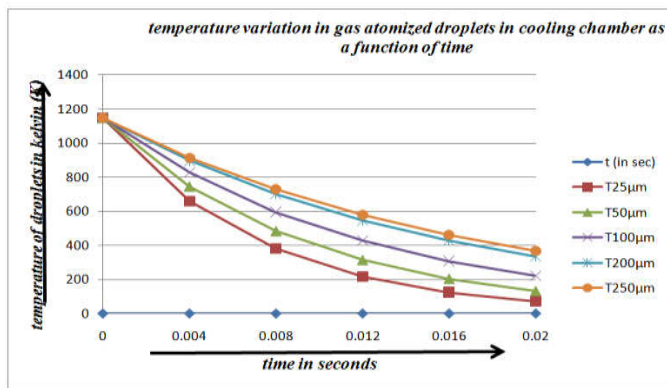


**Figure 4.2.**

Figure 4.3 shows the temperature variation in gas atomized droplets as a function of flight distance it is needed to calculate the cooling rate in K/s.
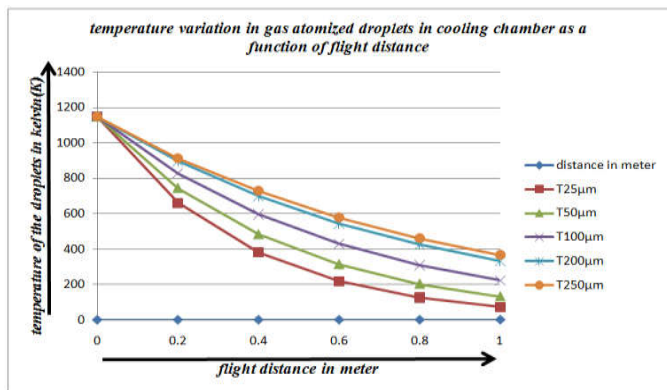


**Figure 4.3**

**Validation of figure 4.2 and figure 4.3**

Studying the figure 4.2 and from the past work done on the same topic we can say that the given graph can be validated. The temperature of the smaller droplets in cooling chamber decreases sharply as compare to bigger droplets because the area to volume ratio of smaller droplets is large and thus heat transfer rate is very fast in smaller droplets, where as larger droplets takes lager time to cool down.

**Application of figure 4.2**

This graph can be used to determine that in cooling chamber what time and with what temperature droplets are striking the substrate. This graph can also be used to set the initial velocity of atomization gas as it was found out from the literature survey it is the initial velocity of the atomization gas that determines the velocity of the droplets.

**Application of figure 4.3**

The graph has its own significance and application for examples using this graph it can be found out at how much distance what size of droplets remains in mushy stage as mushy stage of droplets is the first and the fore most requirements for best quality final product. This graph can also be used to determine the standoff distance, as it can be known using this graph the at what standoff distance how much percentage of droplets and in what range they remains in mushy stage or have solidified fraction between 10 to 90%.

Figure 4.4 shows the cooling rate of different droplet sized in terms of K/s as a function of flight distance.
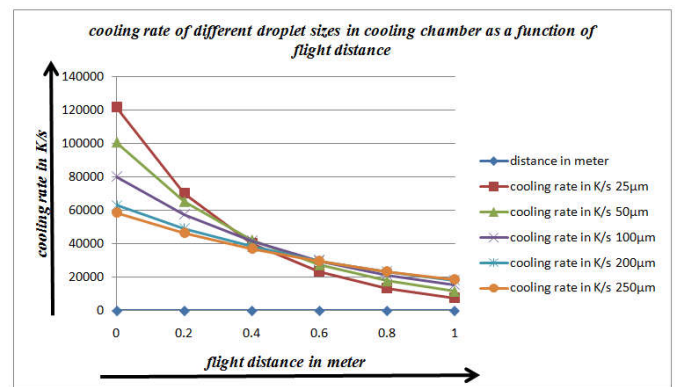


**Figure 4.4**

**Validation and application of Figure 4.4**

It is obvious from the figure that cooling rate in cooling chamber for almost all droplets is of very high value. Although it can be noticed from the figure that initially the smaller droplets has the highest cooling rates in comparison to larger droplets but as the flight distance travelled by the droplets increases the cooling rate for smaller droplets decreases sharply and the cooling rates of larger droplets almost remains constant this is due to the fact that smaller droplets have already lost their heat during the initial stage of heat transfer. The application of cooling rate as a function of flight is to determine what should be the temperature of atomization gas in cooling chamber so that problem of rapid cooling or slow cooling can be solved to achieve the desired cooling rates and thus the desired state of droplets before impacting onto the substrate.

**5. Conclusion**

- The size of the cooling chamber is directly proportional to the flight distance keeping atomizer angle constant.
- The size of the cooling chamber is directly proportional to the atomizer angle keeping keeping flight distance constant.
- The size of the cooling chamber is directly proportional to the size of the droplets.
- The size of the cooling chamber is highly influenced by the reynold number and drag coefficient.

# REFERENCES

Bergmann, D., Fritsching, U. and Crowe, C. T. 2000. "Multiphase flows in the spray forming process," *Proc. 2nd International Conference on Multiphase Flow*, 3–7 April, Kyoto.

Clift R., Grace, J. R. and Weber, M. E. 1978. "*Bubbles, Drops and Particles*", Academic Press, San Diego,CA.

Crowe C. T., Sharma, M. P. and Stock, D. E. 1977. "The particle-source-in-cell method for gas droplet flow", *J. Fluids Engng.,* 99.

Crowe, C. T., Sommerfeld, M. and Tsuji, Y. 1998. "*Multiphase Flows with Drops and Particles*", CRC Press,Boca Raton, CA.

Fritsching, U., Liu, H. and Bauckhage, K. 1991. "Numerical modelling in the spray compaction process", *Proc.5th International Conference on Liquid Atomization and Spray Systems, ICLASS-91*, Gaithersburg,MD, NIST SP813.

Fritsching, U., Liu, H. and Bauckhage, K. 1991. "Two-phase flow and heat transfer in the metal spraycompaction process", *Proc. International Conference on Multiphase Flows,* 24_7 September, Tsukuba.

Grant, P. S., Cantor, B. and Katgerman, L. 1993. *Acta Metall. Mater,* 42.

Gutierrez-Miravete, M., Lavernia, E. J., Trapaga, G. M. and Szekely, J. 1988. "A mathematical model of theliquid dynamic compaction process", *Int. J. Rapid Solidification.*

Lavernia E. J., Gutierrez, E. M., Szekely, J. and Grant, N. J. 1988. "A mathematical model of the liquid dynamic compaction process and heat flow in gas atomization", *Int. J. Rapid Solidification.*

Lawley A., Mathur P., Apelian, D. and Meystel, A. 1990. "Sprayforming: process fundamentals and control," *Powder Metall.* 34.

Lee E. and Ahn S. 1994. "Solidification progress and heat transfer analysis of gas atomized alloy dropletsduring spray forming", *Acta Metall. Mater.,* 42.

Levi C. G. and Mehrabian, R. 1982. "Heat flow during rapid solidification of undercooled metal droplets", *Metall. Trans. A: Phys. Metall. Mater. Sci.* 13A.

Mahesh, N S., Johnson Mendonca, M K Muralidhara, B K MuralidharaAnd C Ramachandra, 2003. "Modeling of droplet dynamic and thermal behaviour during spraydeposition".

Mathur.P., Annavarapu, S., Apelian, D. and Lawley, A. 1989b. "Process control, modeling and applicationsof spray casting", *J. Metals,* 41.

Mathur.P., Annavarapu, S., Apelian, D. and Lawley, A. 1991. "Spray casting: an integral model for processunderstanding and control", *Mater. Sci. Engng.,* A142, 261–70

Ojha S. N., Tripathi, A. K. and Singh, S. N. 1992. "Spray atomization and deposition of an Al–4Cu–20Pballoy", *Powder Metall. Int.,* 25.

Ottosen P. 1993. "Numerical simulation of spray forming", PhD thesis, Technical University of Denmark.

Payne R. D., Matteson, M. A. and Moran, A. L. 1993. "Application of neural networks in spray formingtechnology", *Int. J. Powder Metall.,* 29.

Sadhal S. S., Ayyaswamy, P. S. and Chung, J. N. 1997. *Transport Phenomena with Drops and Bubbles*, Mechanical Engineering Series, Springer Verlag, New York.

Sirignano,W. A. 1998. *Fluid Dynamics and Transport of Droplets and Sprays*, Cambridge University Press, New York.

Zhang J., Wu, Y. and Lavernia, E. J. 1994. "Kinetics of ceramic particulate penetration into spray atomizedmetallic droplets at variable penetration depth", *Acta Metall. Mater.* 42.

*******